Renal Arteriovenous Transit Times of Technetium-Radiolabeled Chelates

Gary R. Conrad, Carl A. Wesolowski*, Kevin S. Berbaum, Karen C. Jensen†, and Peter T. Kirchner

A noninvasive method was developed for quantitating the distribution of renal arteriovenous transit times of technetium-99m (^{99m}Tc) radiopharmaceuticals. Using this method, the characteristic transit times and amplitudes of the first two components of [^{99m}TC] DTPA or MDP transit through the renal vasculature were calculated. The first component amplitude (A1) was evaluated for its ability to discriminate between 20 hypertensive patients with renovascular disease and 21 normotensive subjects. A1 was compared with three other quantitative indices: the ascending slope of the initial renal time-activity curve, the kidney-to-aorta slope ratio (K/A), and renal size. A1 nearly perfectly separated the hypertensive patients from the normotensive subjects; the ability of A1 to discriminate between these two groups is clearly superior to renal size, the initial renal slope, and K/A. We conclude that measurements of the intrarenal distribution of blood flow have distinct advantages over indices of renal blood flow that have been derived from scintillation camera measurements of ^{99m}Tc radiopharmaceuticals.

J Nucl Med 28:1134–1143, 1987

The initial 45 sec of a technetium-99m diethylenetriaminepentaacetate ([^{99m}Tc] DTPA) renogram can be termed the vascular phase of the renogram. Numerous curve parameters, e.g., the slope of the initial rising portion of the renogram, have been proposed to quantitate this vascular phase (*1–4*).

Because renal blood flow determines the initial rate of accumulation of tracer activity within the kidney (*5*), theoretically the early rising portion of the renogram should be proportional to renal blood flow. Based on this hypothesis, Ford et al. (*3*) induced unilateral stenoses in 13 dogs, injected [^{99m}Tc] DTPA as an intravenous bolus, and then measured the slope of the initial rising portions of the renal time-activity curves (TACs); they demonstrated good correlation ($r = 0.93$) between relative renal blood flow, as measured by electromagnetic flow probe or microspheres, and relative curve slopes, expressed as a ratio of right to left.

Although the right-to-left slope ratio reflects changes in relative renal blood flow (*3*), changes in the initial slope of the individual ^{99m}Tc renograms do not always reflect changes in individual renal blood flow (*6*). This variability in the rising slope probably results from the influence of the injection bolus. Kirchner et al. (*1*) attempted to compensate for such bolus effects when they developed an empirical perfusion index called the kidney-to-aorta slope ratio (K/A). The K/A is the ratio of the rising slope of the initial renal TAC to the rising slope of the initial aortic TAC. Kirchner et al. (*7*) attempted to validate this index by performing mechanical renal arterial constriction in six dogs, and by measuring renal blood flow with a flow probe. They reported that K/A was proportional to renal blood flow "whenever the aortic TAC was of good quality"; evidently, the K/A is still dependent on the characteristics of the bolus injection.

In an attempt to derive a reliable, noninvasive measurement of individual renal perfusion, we examined further the relationship between renal and aortic TACs derived from rapid-sequence scintillation camera images following the peripheral venous injection of [^{99m}Tc] DTPA. Based on published observations concerning invasive dye dilution (*8–10*) and radiolabeled colloid washout studies (*11*), we developed a compartmental model of the early vascular transit of radiolabeled che-

Received Jan. 3, 1986; revision accepted Jan. 30, 1987.

For reprints contact: Gary R. Conrad, MD, Dept. of Radiology, CC702 GH, The University of Iowa Hospitals and Clinics, Iowa City, IO 52242.

* Present address: Dept. Nuclear Medicine, General Hospital, Health Science Centre, St. John's, Newfoundland AIB 3V6.

† Present address: Dept. Radiology, Dartmouth-Hitchcock Medical Center, Hanover, NH 03756.

late through the kidney (*12*). Based on this model, we developed a computer-assisted, curve-stripping method for quantitating the distribution of renal arteriovenous transit times (*13,14*). The characteristic transit times (T1, T2) and relative amplitudes (A1, A2) of the first two components, respectively, of radiolabeled tracer transit can be measured using this method. Presumably, these measurements reflect the intrarenal distribution of blood flow (*9–11*).

The purpose of this initial study was to compare A1 to K/A and to the rising slope of the renal TAC, and to determine the ability of each index to discriminate between hypertensive patients with extrinsic renovascular disease and normotensive control subjects. This study also sought to determine if any one of these three indices was superior to renal size as a discriminator between the hypertensive patients and the normotensive subjects.

MATERIALS AND METHODS

Selection of Patients and Control Subjects

The hypertensive population consisted of 20 patients with renovascular disease (five males, 15 females; age range 26–74 yr, mean age 55 yr); each patient underwent renal scintigraphy, renal vein renin sampling, and arteriography. Nine patients had elevated BUN and serum creatinine. One patient had unilateral pelvoureteral duplication and minimal lower-pole caliectasis, as diagnosed by retrograde pyelography; none of the other patients had evidence of acute or chronic renal disease coexisting with the renovascular disease.

Selective renal vein catheterizations were attempted for each patient, and simultaneous renal vein and aortic renin samples were drawn. Abdominal aortography was performed; in selected cases aortography was supplemented with direct renal arterial injections. The results of the renin assays were expressed as the (vein-aorta)/aorta ratio [(V-A/A] (*15*). The severity of the renal arterial stenosis was judged as the maximum percent reduction in lumen diameter, as estimated in the anteroposterior projection.

The normotensive control population consisted of 18 patients referred for bone scintigraphy for nonsystemic orthopedic problems (the most common problem being a stress-related injury) and three physician volunteers (14 males, seven females; age range 17–58 yr, mean age 28). These patients had normal urinalysis, BUN, and serum electrolytes, creatinine, and urate. None of the control patients or volunteers had a history of previous renal disease, renal trauma, or recurrent urinary tract infection.

Imaging Protocol

The 18 normotensive control patients received [^{99m}Tc] methylenediphosphonate (MDP); the three physician volunteers and the 20 hypertensive patients received [^{99m}Tc] DTPA. The imaging protocol was the same for each individual: the subject was placed in the supine position and an upper-extremity peripheral vein was cannulized with an 18- or 21-gauge needle connected to an 85-cm, saline-filled, i.v. extension tube. Using a three-way stopcock, 20 mCi (740 MBq) of ^{99m}Tc radiolabeled chelate was injected into the extension tube; the radiopharmaceutical was surrounded by air bubbles. The extension tube was then flushed with a 10-ml bolus of normal saline. Following the appearance of activity in the lungs, rapid sequence images were acquired in a 64 × 64 byte-frame mode at 1 frame per sec for 50 sec. These scintillation camera images were recorded in the posterior projection using a LEAP collimator mounted on a large field-of-view detector.

Region-of-Interest and Curve Generation

The scintigraphic studies were processed in random order by a physician who had no knowledge of the angiographic findings. The frame of earliest aortic activity was identified and the subsequent 20 frames were added to form a composite image. Four regions-of-interest (ROIs) were drawn over this composite image: aortic, background, and right and left renal.

The abdominal aortic ROI was manually drawn from the level of the lateral costophrenic angles to the approximate level of the renal arteries. Great care was taken to confine the aortic ROI to the projected aortic width; the width of this ROI rarely exceeded 2 pixels. Each renal ROI was manually drawn to encompass as much of the renal parenchyma as possible without exceeding the perceived renal margin. These posterior projection renal areas were used as indices of renal size in the statistical analysis described below. Finally, with the assistance of an isocontour routine,* the background ROI was created by selecting 100–200 of the lowest-count pixels that were located in the lower abdomen. For each ROI, TAC were generated from 40 sequential, 1-sec image frames, beginning 5 frames before the first appearance of activity in the abdominal aorta.

Derivation of Curve Indices

Slope. Assuming that the initial rate of increase in renal activity is constant for at least 3 sec (*2*), three to four points were chosen over the most linear section of the initial upstroke of the renal TAC. A linear fit (by the least squares method) was performed between these manually selected points (*3*), and the slope of this fit line was recorded.

Kidney-to-aorta slope ratio. The aortic slope was obtained from a linear fit to manually selected points on the aortic TAC in the same manner that the renal slope was obtained from the renal TAC. The K/A was recorded as the ratio between the renal slope and the aortic slope, multiplied by the ratio between the aortic region size and the renal region size (*1*).

Component amplitudes and mean transit times. Using a curve-stripping method, T1, T2, A1, and A2 were derived for each kidney. The analysis was performed with the assistance of an interactive computer program written for a dedicated minicomputer.† The program receives aortic, background, and renal TAC as input, and prints A1, T1, A2, and T2 as output. The algorithm proceeds as follows:

The background TAC is multiplied by a scale factor (Appendix C) and then subtracted from the aortic TAC. The renal and background-subtracted aortic TAC are then smoothed with an integral operator (Appendix A). The smoothed aortic TAC is integrated a second time so that each point on the integrated curve represents the sum of all counts prior to that time.

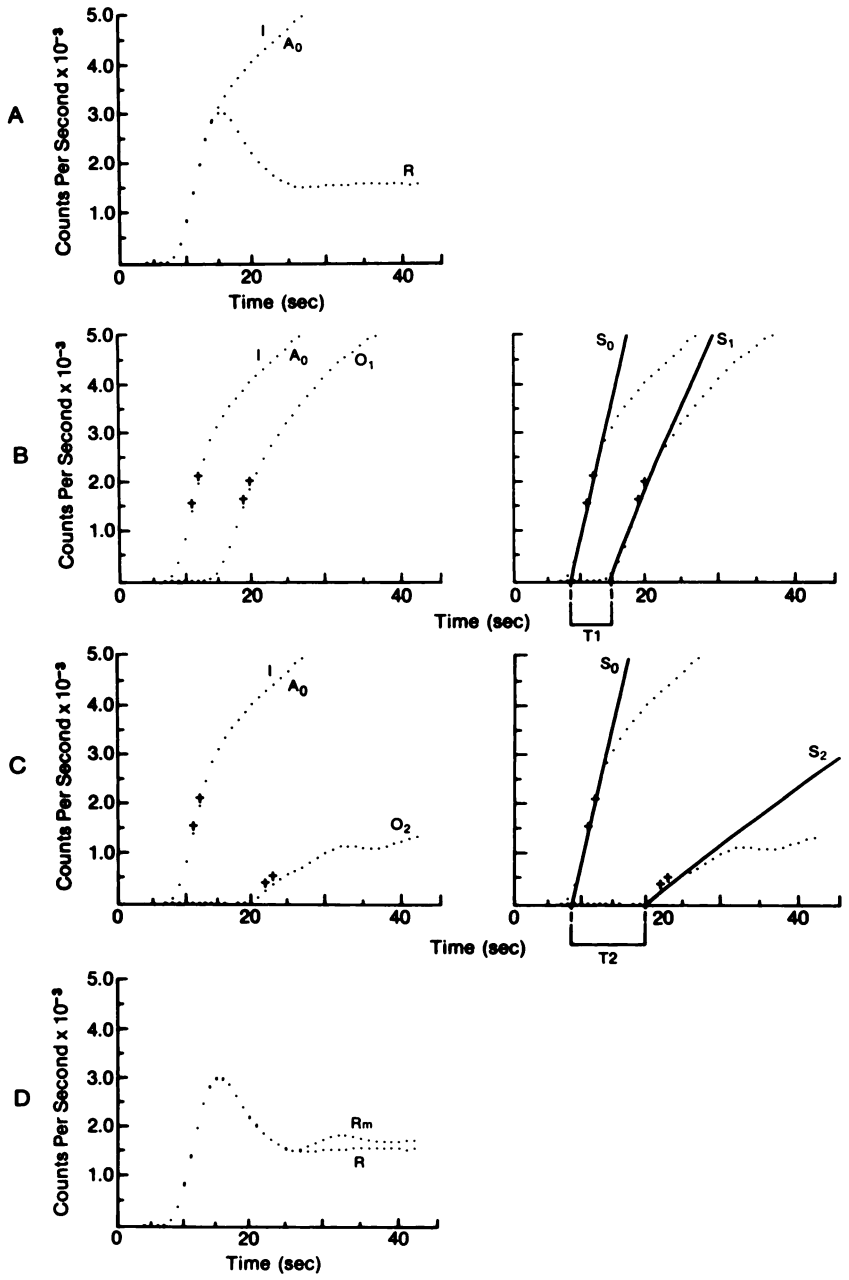

FIGURE 1
Sequence of computer-generated plots used in the derivation of transit time distribution parameters. A: Display of renal TAC and integrated, background-subtracted aortic TAC after scaling and time shifting. The R and I A_0 were obtained from a normotensive subject. B: Derivation of T1 and A1. C: Derivation of T2 and A2. D: Display of renal model curve superimposed over actual renal TAC.

The renal TAC is time shifted and the integrated aortic TAC is *scaled* so that the early portion of the *scaled* integrated aortic TAC (I A_0) matches the early, ascending portion of the time-shifted renal TAC (R) (Fig. 1A). The R is then subtracted from the I A_0 to produce the renal output TAC (O_1).

The operator selects a 2- to 3-point interval on I A_0 where the slope is maximal (with a good injection bolus this interval is easily identified at the first inflection point). The operator designates this curve interval by positioning cursors over the end points (Fig. 1B). A fit line of slope S_0 is drawn through these interval points to intercept the time (t) axis. The operator then selects an interval on O_1 that corresponds to the interval that was marked on I A_0. A fit line of slope S_1 is drawn through this O_1 interval to intercept the t axis. The difference between the t axis intercepts of the two fit lines is an estimate for T1; A1 is calculated as S_1/S_0.

The smoothed aortic TAC now is scaled by the same factor used to scale the integrated aortic TAC. The scaled, smoothed aortic TAC is used to represent the renal input function (P). Based on the compartmental model shown in Figure 2, the following curve is constructed:

$$A1\int_0^t P(\tau - T1)d\tau \qquad (1)$$

Equation (1) represents the contribution of the first component to the total radiolabeled chelate activity that has left the kidney up to t (Appendix B). The curve generated by this equation is stripped from O_1 and the difference curve is labeled O_2; T2 and A2 are derived from O_2 in the same manner as T1 and A1 were derived from O_1 for the first component (Fig. 1C).

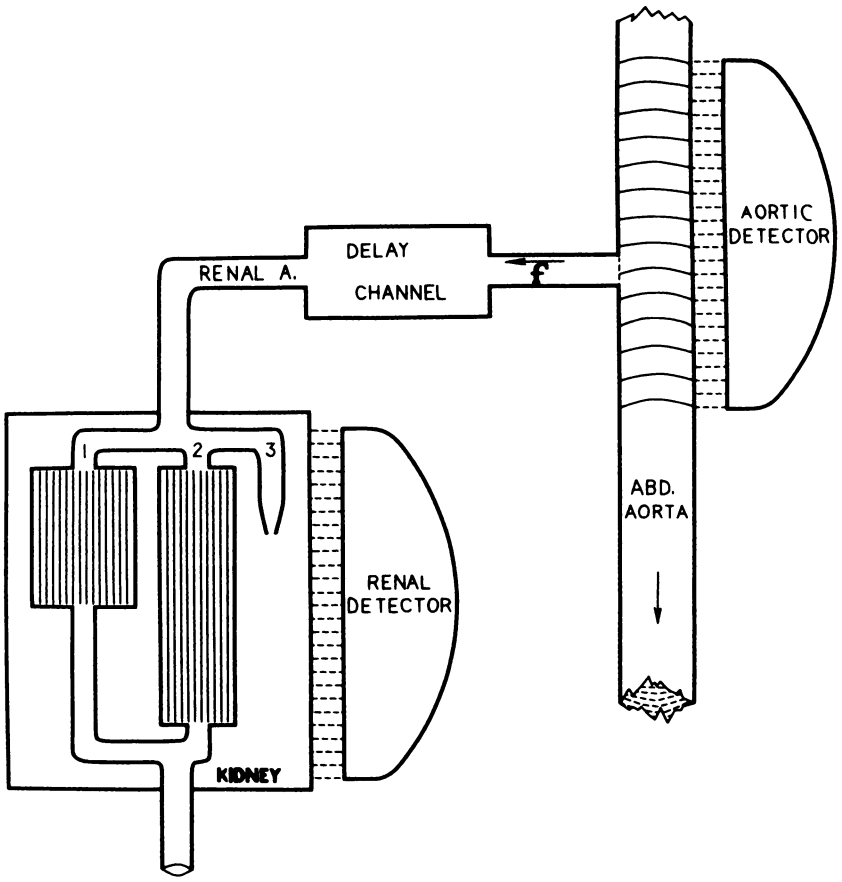

FIGURE 2
Compartmental model of the renal vascular system. Each compartment receives a constant fraction of the renal blood flow. Compartments 1 and 2 function as delay channels and have characteristic transit times. Compartment 3 accounts for the renal extraction of tracer. The renal artery is also modeled as a delay channel; it receives a constant fraction ($\bar{f}$) of the aortic blood flow. Aortic and renal detectors correspond to aortic and renal ROIs, respectively.

After T1, A1, T2, and A2 are computed, the curve-stripping process is discontinued and the renal model curve (R_m) is constructed according to the following equation:

$$R_m(t) = \int_0^t P(\tau)d\tau - A1 \int_0^t P(\tau - T1)d\tau - A2 \int_0^t P(\tau - T2)d\tau \quad (2)$$

The R and R_m are displayed on the same plot (Fig. 1D). If R_m does not adequately fit the early portion of R, then the operator can reenter the program and repeat the analysis using different curve intervals. A single pass requires ~3 min.

Statistical Analysis

Four of the seven renal indices described above were evaluated for their capacity to discriminate between hypertensive patients with renovascular disease and normotensive subjects: (a) size, (b) slope, (c) K/A, and (d) A1. The following analysis was performed for each index:

Mean right kidney and mean left kidney values ($\bar{R}$ and $\bar{L}$, respectively) obtained from the control subjects were compared using Student's t-test (Student's t was calculated from the standard deviation of right-to-left differences). The individual right and left kidney values obtained from the control subjects were also compared using bivariate linear regression analysis (*16*). Based on the slope and intercept of the regression line, a linear transformation was then performed on each left index value (L_i) such that:

$$L_c = (L_i - \bar{L}) \cdot s_r^2 / s_{lr} + \bar{R}$$

where L_c is the transformed (corrected) left value, s_r is the best estimator for the variance σ_r, and s_{lr} is the best estimator for the covariance σ_{lr}.

The statistical analysis was designed to examine the ability of each index to discriminate between individuals with renal disease and individuals without renal disease, rather than between normal and diseased kidneys. For this reason the right index value (R_i) and L_c derived for each patient or control subject were combined into two representative patient values. The first representative value was the minimum of R_i and L_c; the second representative value was the normalized difference between R_i and L_c:

$$\text{normalized difference} = \frac{|L_c - R_i|}{L_c + R_i}.$$

The minimum values obtained for the patients with renovascular disease (n = 20) and the minimum values obtained for the normotensive subjects (n = 21) were plotted as two separate distributions. Receiver-operating-characteristic (ROC) curves were also constructed from these two distributions and the area beneath each ROC curve (P[a]) was calculated using the trapezoidal rule. Each pair of distributions were also compared using the univariate F statistic. The magnitude of the F statistic is a measure of the separation between each pair of distributions. Similarly, P(a) measures the capacity of each index to discriminate between patients with renovascular disease and normotensive subjects (*17,18*).

Difference values were divided into distributions and were analyzed in the manner described above for the minimum values.

RESULTS

Ten of the 20 hypertensive patients with extrinsic renovascular disease had bilateral renal arterial stenoses. The angiographic characteristics of the 30 stenotic renal arteries were categorized as follows: 18 had arteriosclerotic disease, ten had fibromuscular dysplasia, and two had stenoses that could only be classified as "web-like." One of the arteriosclerotic renal arteries had a stenosis of 30%; the remaining arteriosclerotic stenoses ranged from 50% luminal narrowing to total occlusion (the occluded renal arteries had reconstitution of flow from collateral vessels).

Because of technical difficulties, renal vein renins could not be obtained in two of the 20 hypertensive patients; both of these patients had high-grade renal arterial stenoses. Thirteen of the remaining 18 patients had (V-A)/A renin ratios >0.50, either unilaterally or bilaterally. By request of the referring physicians, four of the remaining five hypertensive patients were maintained on propranolol therapy at the time of the renal vein sampling and arteriography. Two of these four patients had unilateral (V-A)/A renin ratios >0.35 and suppression of contralateral renin production; the other two patients had bilaterally suppressed renal vein renins. One additional hypertensive patient with unilateral fibromuscular dysplasia had diminished (V-A)/A renin ratios, but there was no apparent cause for the low values in this patient.

Seven renal indices (size, slope, K/A, A1, A2, T1, and T2) were derived for each of the 21 normotensive control subjects. Table 1 lists the mean and standard deviation of right and left kidney values for each index. The mean T1 for all kidneys (n = 42) was 6.9 sec; T1 ranged from 5.2 to 9.3 sec. The mean T2 for all kidneys was 12.7 sec; T2 ranged from 8.4 to 25 sec. According to Student's t-test, mean left kidney values for slope, K/A, A1, and T1 were significantly greater than the corresponding mean right kidney values. These right–left differences justified the correction of left index values before they were used in the comparison analysis.

TABLE 1
Renal Indices for the Normotensive Control Population (n = 21)

Index	Right kidney*	Left kidney*	t	p
Size, pixels	105 ± 21	112 ± 20	1.69	0.106
Slope, count/sec	329 ± 126	421 ± 145	5.94‡	0.000
K/A	0.78 ± 0.20	0.94 ± 0.25	6.51‡	0.000
Amplitudes				
A1	0.65 ± 0.09	0.69 ± 0.09	3.49†	0.002
A2	0.14 ± 0.09	0.18 ± 0.10	1.69	0.109
Mean transit times				
T1, sec	6.7 ± 1.0	7.0 ± 1.0	3.57†	0.002
T2, sec	12.4 ± 2.2	13.0 ± 3.8	0.69	0.498

* Mean ± s.d.
† $p < 0.007$ test-wise; $p < 0.05$ experiment-wise.
‡ $p < 0.001$ test-wise; $p < 0.01$ experiment-wise.

TABLE 2
Minimum Values of Curve Indices for the Control Population and the Population of Hypertensive Patients with Renovascular Disease

Index	Normotensives* (n = 21)	Hypertensives* (n = 20)	Univariate F†	p
Size	94 ± 24	71 ± 31	7.4	0.0098
Slope	302 ± 124	113 ± 104	27.8	0.0000
K/A	0.74 ± 0.19	0.36 ± 0.16	49.3	0.0000
A1	0.62 ± 0.10	0.25 ± 0.14	99.6	0.0000

* Mean ± s.d.
† Multivariate F is significant.

Four of the seven renal indices (size, slope, K/A, and A1) were compared for their capacity to discriminate between hypertensive patients with renovascular disease and normotensive subjects. Figure 3A shows the distributions of minimum values obtained from the patients with renovascular disease and the control subjects, and lists the P(a) for each index. (The patient whose A1 value fell within the normal range had a unilateral 30% arteriosclerotic stenosis.) Table 2 lists the magnitudes of the F statistics derived for each pair of distributions. According to their ability to discriminate between the two populations, the four indices are ranked as follows: A1 > K/A > slope > size.

The normalized difference value is a measure of renal asymmetry. Figure 3B shows the distributions of normalized difference values obtained for the patients with renovascular disease and the control subjects; Table 3 lists the F statistics derived for each pair of distributions. According to the F statistics, the patients with renovascular disease had no less symmetry in renal size than did the normotensive subjects; however, slope, K/A, and A1 values obtained from these patients were significantly less symmetrical than the corresponding index values obtained from the normotensive subjects. The P(a)s listed in Figure 3B also measured the capacity of each index, based on renal asymmetry, to discriminate between the hypertensive patients and the normotensive subjects. According to their ability to discriminate between the two populations, the four indices are ranked as follows: A1 > slope > K/A > size.

DISCUSSION

Model of the Arteriovenous Transit of an Indicator

Previous investigators have clearly demonstrated that in humans (*9,10*) and in dogs (*8,11*), the renal arterio-

venous transit of an indicator is distributed into two main components. The disadvantage of these published methods for measuring the early venous clearance of radiolabeled colloid (*11*) or opaque dye (*8–10*) is that the indicator must be injected intraarterially.

Our study presents a noninvasive method for measuring the transit time distribution of an intravenously injected radiolabeled tracer. This method is based on a renal vascular model that contains two flow compartments (Fig. 2). The model does not attempt to account for concentration gradients that can develop along the cross section of a vessel; instead, the model assumes that plug flow is present in all vessels (*12,19*).

The model is best understood by imagining how an impulse of blood-soluble tracer might transit the kidney. After being injected into the abdominal aorta, a fraction of the tracer flows into the renal artery; after a short time delay, the tracer enters the kidney. Upon entering the kidney the tracer distributes among three compartments. The first two compartments act as delay channels; these delay channels determine the time at which tracer exits the kidney via the renal vein. The third compartment acts as an accumulator; this compartment accounts for tracer that remains within the kidney during the entire period of observation. The fraction of tracer that entered each compartment can be measured by observing the times at which activity leaves the kidney.

Although a sudden intravenous or intraarterial injection of a radiolabeled tracer does not produce an impulse of activity, sudden injections can be treated as if they were composed of a series of impulses. Provided that the infusion of tracer is not constant, and provided that the transit times through the two compartments are sufficiently different, the components can be separated; once separated, T1, T2, A1, and A2 can be measured.

Using an indicator–dilution method that required the intraarterial injection of an opaque dye and the continuous collection of renal venous blood, Reubi et al. (*10*) measured normal human T1 ranging from 5.0 to 10.9 sec, and T2 ranging from 19.0 to 25.0 sec; these values compare favorably with the T1 and T2 measured in our study using [^{99m}Tc] MDP or [^{99m}Tc] DTPA. However, the ratio between the mean A1 and the mean A2 derived from our normotensive population was 4.2:1 (Table 1), whereas, the ratio between the mean A1 and the mean A2 reported by Reubi et al. (*10*) was 6.1:1. The reason for this discrepancy might be related to differences in methodology, since Reubi et al. stated that their method for measuring A2 was only semiquantitative.

Previously, Rosen et al. (*20*), and later Blaufox et al. (*21*), injected xenon-133 into normal human renal arteries and measured the washout distribution of the noble gas using an external scintillation detector. Rosen et al. obtained a mean A1 to mean A2 ratio of 3.3:1; Blaufox et al. obtained a mean A1 to mean A2 ratio of 4.6:1. Considering the differences in the early renal extraction of xenon (*22*), compared with [^{99m}Tc] DTPA or MDP (*23*), and considering the completely different methods of analysis, the normal A1 to A2 ratios obtained with the radioxenon washout technique are surprisingly similar to the A1 to A2 ratios obtained in our study.

These similarities among amplitudes and transit times support the concept that arteriovenous transit components are distinct physiologic entities. Direct experimental observations of the regional washout of krypton-85 (*24*) and Evan's blue (*8*) from the canine kidney further support this concept. Based on these direct observations, some investigators (*10,11,20,21,25*) have even proposed that the first component of arteriovenous transit represents cortical blood flow, and that the second component represents outer medullary blood flow. However, indicators with different physiochemical properties almost certainly have different anatomic distributions, and A1 and A2 could be influenced by factors unrelated to regional blood flow. A precise correlation between renal model compartments and specific renal histologic structures will require more experimental data.

Statistical Comparison Between A1, K/A, Slope, and Renal Size

Our study sought conclusive data regarding the capacity of A1 to discriminate between hypertensive patients with extrinsic renovascular disease and normotensive individuals without evidence of renal disease. We also sought to compare A1 with vascular-phase indices that previously have been correlated with measurements of renal blood flow. The initial rising slope, K/A, and A1 were derived from the same renal TACs; renal size was based on the renal ROIs used to generate each of these TACs. Although the study patients manifested a broad range of disease severity, all four index values were obtained for each of the 82 kidneys.

Our study was designed not to judge the ability of each index to detect surgically correctable renovascular disease, but merely to determine the ability of each index to discriminate between normal and abnormal individuals. Hypertensive patients with renovascular disease were selected for the abnormal population simply because they were likely to have renal blood flow abnormalities.

For each study individual, R_i was combined with L_c to form two representative index values. The subsequent classification of each individual as normal or abnormal provided the truth data necessary to analyze the variance of these representative values. The histogram plots and ROC curves in Figures 3A and 3B graphically illustrate the variance of each index and

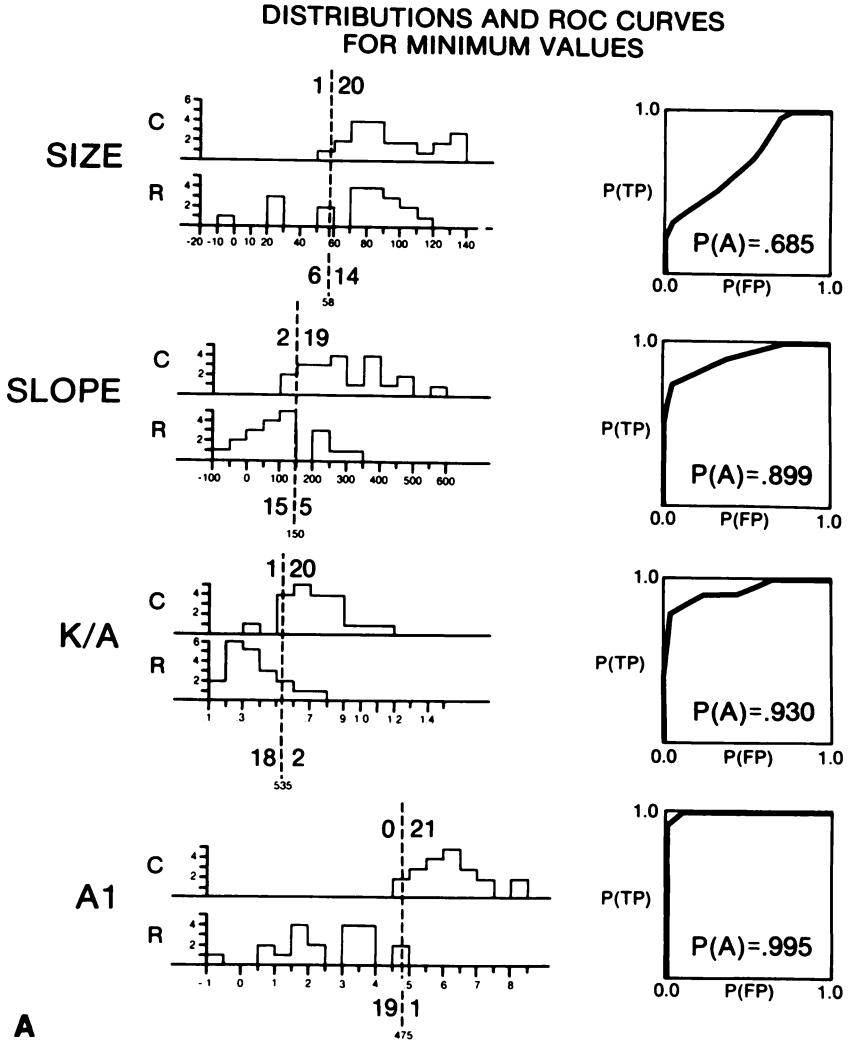

FIGURE 3
Frequency distributions of representative index values obtained from the normotensive control subjects (C) and the hypertensive patients with renovascular disease (R). A: Distributions of minimum values for size, slope, K/A, and A1. B: Distributions of normalized difference values for these indices. Numbers above and below each distribution comprise the decision matrix at the best cut point (vertical dashed line). ROC curves and P(a)s derived from each pair of distributions are included in the right columns.

show how well the representative values derived from hypertensive patients with renovascular disease were separated from the values derived from the normotensive subjects.

The first representative value formulated for each individual was the minimum of R_i and L_c. The minimum values of A1 obtained from the hypertensive patients were almost perfectly separated from the minimum values of A1 derived from the normotensive individuals. Such near-perfect separation is to be *expected*, because these two populations differ with respect to mean age and the presence of renal disease. However, the minimum values of size, slope, and K/A obtained from the hypertensive patients overlapped with the values obtained from the normotensive individuals. Evidently size, slope, and K/A have greater variability than A1. As previously explained, the variability in slope and K/A parameters could result from routine variations in the quality of the injection bolus. Because A1 is derived from an analysis of the renogram in terms of the aortic input function, A1 should be independent of these routine variations in the characteristics of the bolus.

TABLE 3
Difference Values of Curve Indices for the Control Population and the Population of Hypertensive Patients with Renovascular Disease

Index	Normotensives* (n = 21)	Hypertensives* (n = 20)	Univariate F†	p
Size	0.11 ± 0.06	0.19 ± 0.24	2.4	0.1275
Slope	0.08 ± 0.07	0.34 ± 0.34	11.6	0.0016
K/A	0.05 ± 0.03	0.16 ± 0.18	8.3	0.0065
A1	0.04 ± 0.04	0.23 ± 0.23	14.0	0.0006

* Mean ± s.d.
† Multivariate F is significant.

The second representative index value formulated for each individual was the normalized difference between R_i and L_c. The normalized difference value is a relative renal measurement; indices of relative renal blood flow, e.g., the right-to-left slope ratio (*3*), should not be influenced by the quality of the injection bolus. However, the capacity of the normalized difference value to

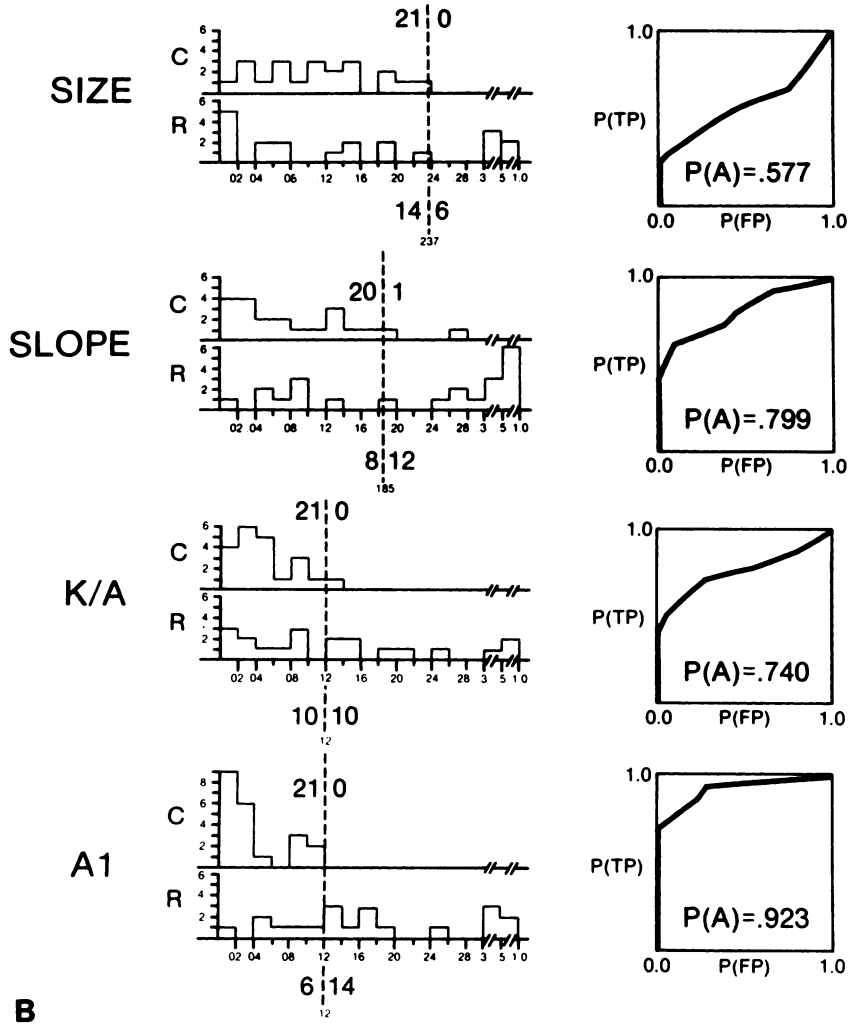

discriminate between patients with hypertensive renovascular disease and normotensive individuals is distinctly less than the capacity of the minimum value, at least for the indices currently studied. This poor performance by the normalized difference value might be explained by the high frequency of bilateral disease in the hypertensive population.

Because the normalized difference values of slope and K/A still were not as well separated as the normalized difference values of A1, factors other than bolus effects must contribute to the variability of slope and K/A. One factor that could contribute to the variability of these two indices is the attenuation of renal activity. Although slope and K/A are susceptible to variations in the attenuation of activity caused by differences in renal depth (*26*), A1 should be independent of this factor. For A1, this attenuation factor should be eliminated during curve analysis when the integrated aortic TAC is scaled to match the early renal TAC.

Since renal size, slope, and K/A did not cleanly separate the two distinct populations examined in our study, they have little potential for separating other abnormal populations. Not surprisingly, Keim et al. (*2*) reported that renal size and K/A did not reliably separate patients with renovascular hypertension from patients with essential hypertension.

Although A1 appears to be an excellent discriminator between hypertensive patients with renovascular disease and normotensive subjects, more data will be required to determine if any of the transit time distribution parameters have clinical applicability. Since most hypertensive screening populations have a low prevalence of renovascular disease (*2,27*), a large hypertensive population will need to be studied in order to determine if A1 can reliably predict surgically "curable" renovascular hypertension (*15,28*). Considering the preliminary data obtained in our study, the collection of such a prospective series seems warranted.

APPENDIX

Theoretical Basis for Measuring Component Amplitudes and Transit Times from the Renogram

Symbol definitions

- t = time (origin corresponds to time of first arrival of tracer)
- ω = time constant for integral operator ξ
- μ = sampling time (reciprocal of framing rate)
- T_i = characteristic transit time of the *ith* component
- A_i = amplitude of the *ith* component
- ϵ = time delay between R and A_0
- k = proportionality constant relating R to A_0
- b = proportionality constant relating A_0 to B
- λ = decay constant
- $f(t)$ = input
- $F(t)$ = integral of input
- $g(t)$ = output
- $G(t)$ = integral of output
- $h(t)$ = system response to unit impulse
- $q(t)$ = retention (corresponds to quantity of tracer in kidney)
- $P(t)$ = activity that results from radiolabeled tracer entering the kidney through the renal artery or arteries. P(t) represents activity (counts per unit time) observed during a time interval equivalent to the sampling time
- $R(t)$ = renal activity as measured by renal ROI
- $A_0(t)$ = aortic activity as measured by aortic ROI
- $B(t)$ = background activity as measured by background ROI

A. *Integral operator.* Given a continuous function $f(t)$, the integral operator ξ is defined as:

$$\xi(f,\omega) = \int_{t-\omega}^{t} f(\tau)d\tau$$

The ξ operator defines the effect of sampling a tracer function f for a duration of $\omega = \mu$. The ξ operator also is used as an asymmetric smooth.

B. *Output and retention functions.* The renal vascular system can be modeled as a linear physical system comprised of m non-mixing delay channels. In this model, each channel is characterized by a unique transit time t_j, and each channel receives a fraction h_j of the total tracer that enters the system. We define this system to be stable if $\{h_j, t_j\}$ are constants and

$$\sum_{j=1}^{m} h_j = 1$$

Under these conditions, the relationship between the cumulative input F(t) and the cumulative output G(t) of tracer is:

$$G(t) = \sum_{j=1}^{m} h_j \cdot F(t - t_j)$$

The logical extension of this discrete delay-channel model is an incremental form in which $t_{j+1} - t_j$ approaches 0 as m approaches infinity in the limit. Thus,

$$G(t) = \int_0^{\infty} h(\tau)F(t - \tau)d\tau.$$

With this incremental form, the assumption of non-mixing is relaxed but the system still is assumed to be linear and stationary (*19*). Now let us confine our discussion to experiments utilizing sudden injections, where $F(t) = 0$ for $t \leq 0$. According to published experiments that have utilized such injections (specifically, intraarterial injections), the system response appears to consist of two or more components (*9–11*). Such observations suggest that h(t) can divided into n intervals $[T_i', T_{i+1}']$, for i = 1,n. The output attributable to the *ith* interval is then:

$$G_i(t) = \int_{T_i'}^{T_{i+1}'} h(\tau)F(t - \tau)d\tau. \quad (3)$$

Analogous to this division of the system response into multiple components, the discrete form of the delay-channel model can be organized into multiple compartments, each compartment would then represent a group of delay channels with similar transit times. This simplification of the delay-channel model suggests that following approximation to Eq. (3):

$$G_i(t) \simeq A_i \cdot F(t - T_i),$$

where $\{A_i, T_i\}$ are constants, $T_i' < T_i < T_{i+1}'$, and

$$\sum_{i=1}^{n} A_i = 1$$

Therefore, since $q(t) = F(t) - G(t)$, then

$$q(t) \simeq \int_0^t f(\tau)d\tau - \sum_{i=1}^{n} A_i \int_0^t f(\tau - T_i)d\tau. \quad (4)$$

Equation (4) applies to a large number of tracers. To account for the sampling of radiolabeled tracers, let $R(t) = \lambda\xi(q, \mu)$ and let $P(t) = \lambda\xi(f, \mu)$. Thus,

$$R(t) \simeq \int_0^t P(\tau)d\tau - \sum_{i=1}^{n} A_i \int_0^t P(\tau - T_i)d\tau. \quad (5)$$

After application of the integral operator, the right side of Eq. (5) is equivalent to R_m in Eq. (2), for n = 2. Both Eqs. (2) and (5) describe the simplified model that is diagramed in Figure 2. The qualitatively close fit that is usually obtained between R_m and the early portion of the renal TAC demonstrates the utility of this simplified delay-channel model (Fig. 1).

C. *Input function.* The tracer bolus reaching the abdominal aorta is so broad and the aortic velocity is so great that the aortic ROI does not appreciably integrate the bolus signal (*29*). Furthermore, for $t < T_1'$, the properly time-shifted renal TAC is proportional to the integral of the aortic TAC. These observations suggest the following approximate derivation of the activity function P(t) from the aortic TAC:

$$P(t) \simeq k\,[A_0(t - \epsilon) - bB(t - \epsilon)]. \quad (6)$$

The rationale for subtracting background activity from the abdominal aortic TAC comes from a dog model in which an arteriovenous femoral catheter was exteriorized and coiled beneath a scintillation camera (Hornof WJ, D.V.M., unpublished data, 1985). Data acquisition following the intravenous bolus injection of [^{99m}Tc] DTPA permitted the generation of TACs corresponding to catheter, abdominal aorta, and abdominal background ROIs. The background TAC, when scaled and added to the loop TAC, mimicked the aortic TAC. For human data, an empirical estimate of this scale is given by:

$$b = \frac{0.8\ A_0(t_m)}{B(t_m)} \cdot \frac{2\ B(t_{40})}{A_0(t_{40})},$$

where t_m is the time at which

$$A_0(t) - B(t) \cdot \frac{A_0(t_{40})}{2\ B(t_{40})}$$

is a minimum for $t \leq 40$ sec. The precise method of selecting b is actually not critical to the determination of k. However, the background subtraction indicated by Eq. (6) does improve the linear relationship between the time-shifted renal TAC and integrated aortic TAC.

NOTES

* Medical Image Processing Specialists, Inc., Ann Arbor, MI.

† Medical Data Systems A2/A3.

ACKNOWLEDGMENTS

The authors thank Clare Chon for her technical assistance, and Dr. William Hornof for his critical review of the manuscript.

REFERENCES

1. Kirchner PT, Goldman MH, Leapman SB, et al. Clinical application of the kidney to aortic blood flow index (K/A ratio). *Contrib Nephrol* 1978; 11:120–126.
2. Keim HJ, Johnson PM, Vaughan ED, et al. Computer-assisted static/dynamic renal imaging: a screening test for renovascular hypertension? *J Nucl Med* 1979; 20:11–17.
3. Ford K, Harris CC, Coleman RE, et al. The radionuclide renogram as a predictor of relative renal blood flow. *Radiology* 1983; 149:819–821.
4. Nally JV, Clarke HS, Windham JP, et al. Technetium-99m DTPA renal flow studies in Goldblatt hypertension. *J Nucl Med* 1985; 26:917–924.
5. Bassingthwaighte JB, Holloway GA. Estimation of blood flow with radioactive tracers. *Semin Nucl Med* 1976; 6:141–161.
6. Köenigsberg M, Novich I, Lory M, et al. Detection of asymmetrical renal perfusion by radiopertechnetate angiography. *J Nucl Med* 1974; 15:507.
7. Kirchner P, Gray F, Short D, et al. Correlation of gamma camera and flow meter determined renal blood flow measurements. *J Nucl Med* 1974; 15:506–507.
8. Kramer K, Thurau K, Deetjen P. Hämodynamik des nierenmarks. *Pflügers Arch* 1960; 270:251–269.
9. Reubi FC, Gossweiler N, Gurtler R, et al. Methods of measuring renal circulation in man. In: Proceedings of the 2nd International Congress in Nephrology. Prague, 1963, pp. 78–83.
10. Reubi FC, Gossweiler N, Gurtler R, et al. Renal circulation in man studied by means of a dye-dilution method. *Circulation* 1966; 33:426–442.
11. Mitchell TG. Measurement of intrarenal blood flow. *Fed Proc* 1963; 22:218.
12. Wesolowski CA, Conrad GR, Kirchner PT. A direct modeling approach to the early renal vascular transit of Tc-99m chelates. *Med Phys* (in press).
13. Conrad GR, Wesolowski C, Kirchner PT. Intrarenal blood flow distributions from first transit recordings of Tc-99m radiochelates. *J Nucl Med* 1985; 26:P132.
14. Wesolowski CA, Conrad GR, Kirchner PT. A renal vascular transit time distribution method for use with technetium-99m compounds. *J Nucl Med* 1986; 27:P1006–1007.
15. Sos TA, Vaughan ED, Pickering TG, et al. Diagnosis of renovascular hypertension and evaluation of "surgical" curability. *Urol Radiol* 1982; 3:199–203.
16. Deim K, Lentner C, eds. Scientific tables. New York: Ciba-Geigy, 1970:179–183.
17. Winer AJ. Statistical principles in experimental design. New York: McGraw Hill, 1971:149–257.
18. Hayes WL. Statistics, 3rd ed. New York: Holt, Rinehart, and Winston, 1981:325–412.
19. Gonzalez-Fernandez JM. Theory of the measurement of the dispersion of an indicator in indicator-dilution studies. *Circ Res* 1962; 10:404–428.
20. Rosen SM, Hollenberg NK, Dealy JB, et al. Measurement of the distribution of blood flow in the human kidney using the intra-arterial injection of Xe-133. *Clin Sci* 1968; 34:287–302.
21. Blaufox MD, Fromowitz A, Gruskin A, et al. Validation of use of xenon-133 to measure intrarenal distribution of blood flow. *Am J Physiol* 1970; 219:440–444.
22. Ladefoged J, Pedersen F, Doutheil U, et al. Renal blood flow measured with xenon-133 wash-out technique and with an electromagnetic flowmeter. *Pflügers Arch* 1965; 284:195–200.
23. McAfee JG, Grossman ZD, Gagne G, et al. Comparison of renal extraction efficiencies for radioactive agents in the normal dog. *J Nucl Med* 1981; 22:333–338.
24. Thorburn GD, Kopald HH, Herd JA, et al. Intrarenal distribution of nutrient blood flow determined with Kr-85 in the unanesthetized dog. *Circ Res* 1963; 13:290–307.
25. Barger CA. Renal hemodynamic factors in congestive heart failure. *Ann NY Acad Sci* 1966; 139:276–284.
26. Gruenewald SM, Collins LT, Fawdry RM. Kidney depth measurement and its influence on quantitation of function from gamma camera renography. *Clin Nucl Med* 1985; 10:398–401.
27. McNeil BJ, Varady PD, Burrows BA, et al. Cost-effectiveness calculations in the diagnosis and treatment of hypertensive renovascular disease. *N Engl J Med* 1975; 293:216–226.
28. Arlart I, Rosenthal J, Adam WE, et al. Predictive value of radionuclide methods in the diagnosis of unilateral renovascular hypertension. *Cardiovasc Intervent Radiol* 1979; 2:115–125.
29. Wesolowski CA, Hurwitz GA, Conrad GR, et al. The long abdominal aortic region of interest for renal vascular quantitative analyses. *Clin Invest Med* 1986; 9:A118.